Surface & Coatings Technology 295 (2016) 70–77

Contents lists available at ScienceDirect

Surface & Coatings Technology

journal homepage: www.elsevier.com/locate/surfcoat

The adhesion of normal human dermal fibroblasts to the cyclopropylamine plasma polymers studied by holographic microscopy

L. Štrbková [a,*], A. Manakhov [b], L. Zajíčková [b,c], A. Stoica [b], P. Veselý [a,d], R. Chmelík [a,d]

[a] Experimental Biophotonics, CEITEC — Central European Institute of Technology, Brno University of Technology, Technická 3058/10, 61600 Brno, Czech Republic
[b] Plasma Technologies, CEITEC — Central European Institute of Technology, Masaryk University, Kotlářská 2, 61137 Brno, Czech Republic
[c] Department of Physical Electronics, Faculty of Science, Masaryk University, Kotlářská 2, 61137 Brno, Czech Republic
[d] Institute of Physical Engineering, Faculty of Mechanical Engineering, Brno University of Technology, Technická 2896/2, 61600 Brno, Czech Republic

ARTICLE INFO

Article history:
Received 22 May 2015
Revised 25 September 2015
Accepted in revised form 31 October 2015
Available online 2 November 2015

Keywords:
Plasma polymer
Cyclopropylamine
Cell adhesion
Holographic microscopy
Quantitative phase imaging

ABSTRACT

The understanding of cell–surface interactions plays an important role for the biomaterials development and bioengineering. Although it is already known that amine groups increase the cell adhesion and proliferation, the influence of amine layers properties on cell viability is the subject of further investigation. In this work, amine-rich coatings were prepared by low pressure plasma polymerization of cyclopropylamine using radio frequency (RF) capacitively coupled discharge. Normal human dermal fibroblasts were chosen for the monitoring of biological response to the properties of amine layers. As a superior technique for the label-free monitoring of the cell–surface interaction, coherence-controlled holographic microscopy (CCHM) was exploited. CCHM enables quantitative phase imaging. From such images, valuable morphological parameters of cells directly related to the cell dry mass can be extracted. Based on those parameters, viability of cells cultivated on the plasma-treated surfaces with different properties was studied and evaluated. According to the results, amine-rich films enhanced the conditions for the cell adhesion and proliferation.

© 2015 The Authors. Published by Elsevier B.V. This is an open access article under the CC BY-NC-ND license (http://creativecommons.org/licenses/by-nc-nd/4.0/).

1. Introduction

In the past few years, the interaction of cells with engineered biomaterials has been the subject of numerous studies. The investigation of the surface–cell interaction is of great importance for various applications including tissue engineering, wound healing, implants, and cell culture vessels design [1–3]. The properties of a surrounding microenvironment influence the cell migration, proliferation, organization and differentiation [4]. Therefore, the development of biomaterials for the mentioned applications has recently focused on the design of biocompatible structures that are capable of imitating the natural cellular environment [3,5].

The bioapplications of materials with noble bulk properties (e.g. hardness, stability, morphology) are often hindered by their low surface free energy, i.e. poor wettability [6]. Thus, the surface modification of various materials including polymers attracts attention of the community of material scientists [7]. Different processes including self-assembled monolayer (SAM) growth [8], graft polymerization [9], silanization [10], plasma treatment and plasma polymerization [7,11–18] were used to increase the surface free energy by introducing hydrophilic groups (amines, carboxyl, hydroxyl, etc.) at the material surface.

Plasma processes have certain advantages compared to the wet chemical methods of surface modification. First of all, plasma processing is an environment friendly energy-efficient technology because it does not consume solvents. Secondly, it is a substrate-independent technology, i.e. it can be applied to various materials including thermal sensitive polymers. Finally, plasma modification does not affect the bulk properties of materials unlike many wet chemical methods requiring soaking in reactive mixtures, such as piranha solution or KOH. Nevertheless, the deposition of plasma polymers exhibiting a good layer stability combined with the sufficient concentration of functional groups is still challenging [19]. Recently, we have shown that stable amine-rich plasma films can be deposited by plasma polymerization of non-toxic cyclopropylamine (CPA) [20–22]. Although Lee et al. proposed that positively charged amine surfaces enhance the adhesion of fibroblasts not all amine plasma coatings can be applied for biomedical applications [6]. The release of toxic oligomers or a degradation of the plasma coating may negatively affect the biocompatibility of the plasma coated material [23]. The plasma polymers prepared from CPA have never been tested before for their biocompatibility. The viability of cells on these films has to be investigated because it is essential for the optimization of these promising films aimed at the biomedical applications and for a better understanding of amine surface–cell interactions.

* Corresponding author at: Central European Institute of Technology, Brno University of Technology, Technická 3058/10, 61600 Brno, Czech Republic.
E-mail address: lenka.strbkova@ceitec.vutbr.cz (L. Štrbková).

http://dx.doi.org/10.1016/j.surfcoat.2015.10.076
0257-8972/© 2015 The Authors. Published by Elsevier B.V. This is an open access article under the CC BY-NC-ND license (http://creativecommons.org/licenses/by-nc-nd/4.0/).

There are several existing experimental approaches and techniques providing deeper insights into the processes occurring during the interaction of cells with the biomaterials. In the past, mainly simple cell counting, detachment and colorimetric assays were used to analyse the interaction of cells with different materials [24]. These methods do not provide the morphological information and do not allow for a dynamic observation of the cell–surface interaction. In the recent years, electrochemical methods and high-resolution microscopic techniques were applied for the assessment of the biocompatibility of materials [24]. However, the microscopic techniques such as scanning force microscopy (SFM) [25], scanning electron microscopy(SEM) [24], total internal reflection fluorescence microscopy (TIRF) or confocal laser scanning microscopy (CLSM) [4]are either not quantitative, require the labelling of the cells, or have high illumination power, which could influence the sample. In this work, we present the coherence-controlled holographic microscopy (CCHM) as a promising technique which is able to evaluate the biocompatibility of surfaces while overcoming the limitations of the mentioned approaches.

CCHM belongs to the techniques that allow for label-free quantitative phase imaging [26–28]. The imaging in CCHM is based on the interference of the object and the reference light beams, which enables to detect the phase delay of light transmitted through the specimen [29]. When observing the live cells that are considered to be weakly scattering and absorbing specimens, the phase carries considerably more information about the specimen than the amplitude of a transmitted light and is, therefore, of a great significance. Since the images gained by the CCHM carry a quantitative information about the imaged cells, valuable morphological parameters (features) describing the cell behaviour can be obtained from the images. The parameters are directly related to the cell mass [30–33]and, therefore, they are crucial for the assessment of biocompatibility of the surfaces. Moreover, the low illumination power of CCHM (0.2 $\mu W/cm^2$) is not likely to influence the cell behaviour, hence does not affect the results of the analysis.

In this work, the interaction of normal human dermal fibroblasts with the CPA plasma polymers is investigated by CCHM. The morphological cell parameters are obtained from the quantitative phase images and further analysed in order to evaluate the cell–surface interaction. For the first time, the time-dependent evaluation of the cell-amine plasma layer interaction is monitored by the label-free quantitative microscopic technique.

2. Experimental details

2.1. Preparation of samples

The CPA plasma polymers were prepared in a stainless steel parallel plate reactor depicted schematically in Fig. 1. The bottom electrode, 420 mm in diameter, was capacitively coupled to a RF generator working at the frequency of 13.56 MHz. The gases were fed into the chamber through a grounded upper showerhead electrode, 380 mm in diameter. The distance between the electrodes was 55 mm. The bottom electrode with substrates was negatively DC self-biased due to an asymmetric coupling. The reactor was pumped down to 10^{-4} Pa by a turbomolecular pump with a backing rotary pump. The deposition was carried out with the rotary pump only. The leak rate including wall desorption was below 0.1 sccm for all the experiments.

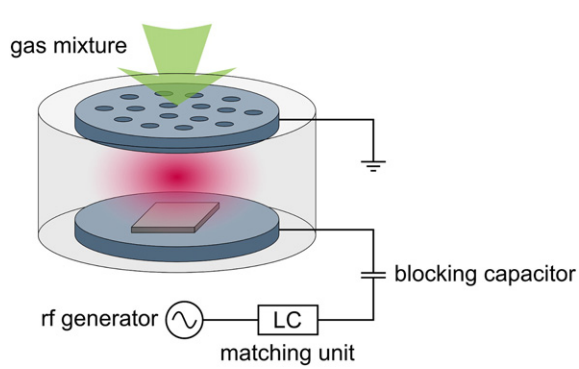

Fig. 1. Schematic drawing of the plasma set-up.

The CPA (98%, Sigma Aldrich) was polymerized in pulsed or continuous CPA/Ar plasmas (Table 1) at a pressure of 50 Pa and on-time power of 100 W. For pulsed mode, the pulse duty cycle and repetition frequency were 33% and 500 Hz, respectively. The bias voltage was in the range from −5 to −10 V. The flow rate of Ar, 28 sccm, was regulated by an electronic flow controller Hastings, whereas the flow rate of CPA vapours, 2.0–2.7 sccm, was set by a needle valve. The deposition time was 60 min. The substrates were sputter-cleaned by pulsed Ar plasma for 10 min prior to the deposition. Double-side polished single crystal silicon (c-Si) wafers (<111>, N-type phosphorus doped, resistance 0.5 Ω cm) supplied by ON-Semiconductor, Czech Republic were used as substrates for the optical and mechanical characterization and XPS analyses. Round shape glass coverslips (P-LAB a.s.) were used as substrates for cell cultivation.

2.2. Characterization of thin films

X-ray photoelectron spectroscopy (XPS) for the surface (6–9 nm) chemical characterization of coated c-Si was carried out using an Omicron non-monochromatic X-ray source (Al Kα, DAR400, output power 270 W) and an electron spectrometer (EA125) attached to a custom built ultra-high vacuum system. No charge compensation was used. The quantitative composition was determined from detailed spectra taken at the pass energy of 25 eV and the electron take off angle of 50°. The maximum lateral dimension of the analysed area was 1.5 mm. The quantification was carried out using XPS MultiQuant software [34]. The software CasaXPS 2.3.16 was used for the fitting of XPS atomic signals using convolutions of 30% Lorentzian and 70% Gaussian profiles. A larger portion of Lorentzian profile led to an improved agreement between the fit and the experimental data but maximum 30% was used as recommended for the fitting of XPS data on polymers by Beamson and Briggs [35]. The FWHM was set in the range 1.8–1.9 eV in order to get the smallest as possible width of the peaks.

The films on c-Si were characterized by ellipsometry using a phase modulated Jobin Yvon UVISEL ellipsometer in the spectral region of 1.5–6.5 eV with angle of incidence of 65°. The data were fitted using a PJDOS dispersion model for SiO_2-like materials and a structural model of wedge-shaped non-uniform thin film [36]. It allowed determining the film thickness, thickness nonuniformity and dispersion parameters determining the spectral dependencies of optical constants. Fourier transform infrared spectroscopy (FT-IR) of the films on c-Si was carried out with Bruker Vertex 80v spectrophotometer in the transmission mode.

A Hysitron TI-950 TriboIndenter equipped with diamond Berkovich indenter was used in the evaluation of the hardness and elastic modulus of the deposited thin films. The nanoscale measuring head with resolution of 1 nN and load noise floor less than 30 nN was used for the measurements. Quasistatic nanoindentation tests with several partial unloading (PUL) segments were performed in the range of indentation loads from 0.1 to 10 mN. The standard Oliver and Pharr [37] approach was used to evaluate the hardness and elastic modulus of the studied films. A series of nine tests with 20 unloading segments were performed in the above mentioned load range at different locations on each sample, as described in our previous work [38]. The in-situ scanning probe microscopy (SPM) imaging using the indenter tip was employed for a precise positioning and surface topography evaluation before and after the tests.

Table 1
Physical parameters of CPA plasma polymers (v_d is deposition rate) in dependence on varying deposition conditions, CPA flow rate (Q_{CPA}) and discharge mode. The fixed deposition conditions were: flow rate of Ar 28 sccm, total pressure 50 Pa, RF power 100 W and deposition time 60 min.

Sample	Q_{CPA} sccm	Discharge mode	v_d nm/min	Thickness loss after 128 h in water %	Hardness		Elastic modulus	
					Before immersion GPa	After immersion GPa	Before immersion GPa	After immersion GPa
CPA40	2.7	Pulsed	5.3	5.6	0.55 ± 0.02	0.44 ± 0.02	13 ± 2	17 ± 6
CPA42	2.0	Continuous	3.4	1.0	–	–	–	–
CPA43	2.0	Pulsed	4.1	2.0	0.58 ± 0.02	0.39 ± 0.02	15 ± 1	12 ± 1

2.3. Cell culture experiments

2.3.1. Cell culture

The normal human dermal fibroblasts (LF cells) were used for cell culture experiments. The cells were maintained in Eagle's minimal essential medium (provided by Institute of Molecular Genetics of the ASCR) supplemented with 10% fetal bovine serum (Sigma-Aldrich) and gentamicin (Sigma-Aldrich) in an incubator at 37 °C and 3.5% CO_2 atmosphere. Cells were then detached with trypsin and seeded into sterilized observation chambers with glass bottom coverslips (two plasma coated coverslips and one control). The seeding densities were 15 cells/mm^2 in order to achieve sparse coverage for the purposes of segmentation of individual cells. The observation chambers were kept in the incubator under the same conditions.

2.3.2. Cell imaging

The samples (control, CPA40, CPA42 and CPA43) were imaged by CCHM at three time instants, 2, 3 and 4 days, after cell seeding (with the interval approximately 24 h). At least 30 images were acquired from each sample at each time point in pursuit of collecting data for the statistical analysis. Images were acquired in a random manner across each sample. While acquiring images for extraction of cell morphological parameters, objectives Nikon 10×/0.3 were used. The imaged area when using these objectives is 379 × 379 μm^2. For the cell count and confluence determination, Nikon 4×/0.1 objectives providing the field of view 947 × 947 μm^2 were used.

CCHM [27,28] was built at Brno University of Technology. The optical set-up of the microscope is based on Mach–Zehnder-type interferometer modified for incoherent off-axis holographic microscopy (Fig. 2) [28].The illumination is formed by a halogen lamp as a low coherence source, interference filters, collector lens and beamsplitter, which splits the beam into two separated nearly identical optical arms — reference and object arms. Both arms contain matching condensers, objectives and tube lenses. The reference arm includes diffraction grating, which spatially separates light of different wavelengths. Only the +1st order beam is separated and interferes with the object beam in the output plane, while creating interference structure — hologram. The hologram is recorded by the CCD camera (XIMEA MR4021MC-VELETA). The imaging characteristics of CCHM are described in detail in [39].

The numerical reconstruction of the hologram is performed using the house-built software based on fast Fourier transform methods [40, 41] and phase unwrapping [42,43]. The reconstructed quantitative phase images acquired by CCHM contain values of phase delays induced by the specimen expressed in radians/pixel.

2.3.3. Evaluation of cell behaviour

Several features (parameters) describing the cell morphology were extracted from the microscopic images for comparison of the cell behaviour on different surfaces. The quantitative phase imaging by CCHM enables to extract cell features that are based on the phase distribution in the cell region and, therefore, provide information about the dry mass density distribution within the cells (see Supporting Information). The example of quantitative phase image used for further analysis is shown in Fig. 3. The cells in the image were firstly segmented by marker-controlled watershed segmentation approach [44]and identified as separate regions by the automatic procedure performed in MATLAB (MathWorks, Inc.). Afterwards, the cell features were extracted from each detected cell region. The set of obtained features was further statistically analysed in STATISTICA (StatSoft, Inc.). The significance

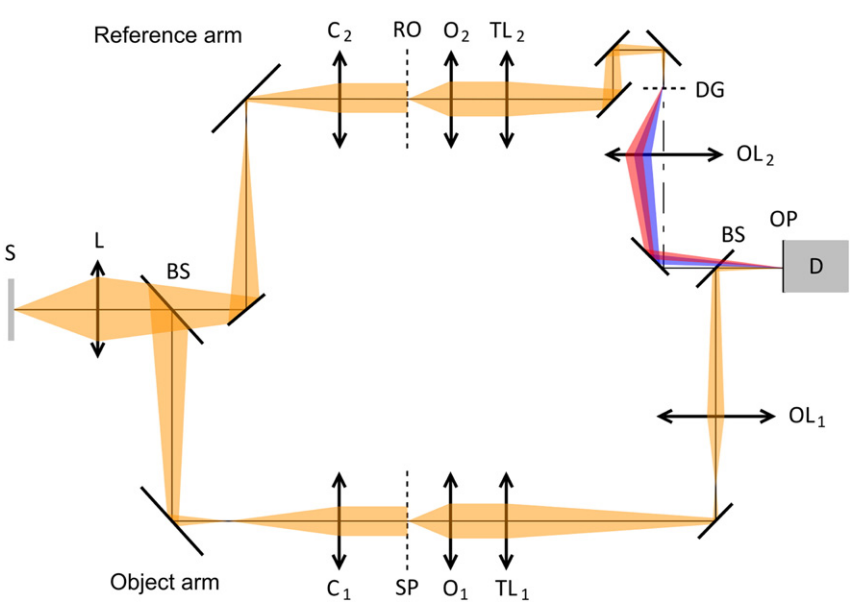

Fig. 2. Optical setup of CCHM. Light source (S), relay lens (L), beamsplitters (BS), condensers (C), specimen (SP), reference object (RO), microobjectives (O), tube lenses (TL), diffraction grating (DG), output lenses (OL), output plane (OP), detector (D) [28].

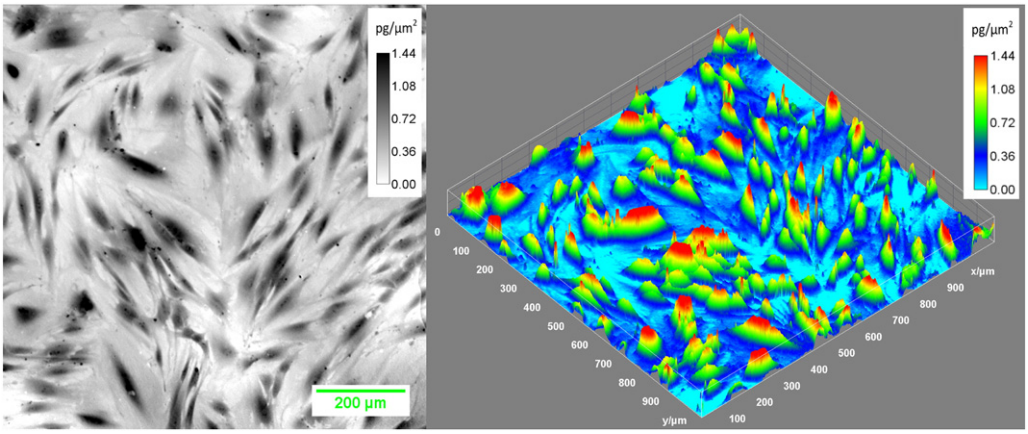

Fig. 3. Quantitative phase image of CPA40 gained by CCHM with objectives 4×/0.1 (left) and its surface plot (right).

of differences between the feature values was tested using an unpaired t-test.

The set of extracted features included: *footprint area*, *average dry mass density*, *total dry mass* and *skewness.* Additionally, the *cell count* and *confluence* were determined. The parameters were calculated automatically using algorithm implemented in MATLAB. The *footprint area* can be calculated as the sum of the pixels of the cell region multiplied by the pixel area. It provides information about the cell spreading and adherence. The *average dry mass density* is calculated as a mean of the dry mass density (see Supporting Information) for each cell region (in picograms over squared micrometres). Dry mass density quantifies the mass of the non-aqueous material of the cell [30–33]. In context with other parameters, average dry mass density reports about the flatness of the cell. The feature *total dry mass* quantifies overall dry mass of the cell (in picograms) and provides information regarding the cell viability. The *skewness* is calculated from histogram of the phase values in the cell region and describes its shape. The *Skewness* measures symmetry of the distribution of the phase values from the mean value in the cell region and therefore provides information about the adherence of the cell. Values of *skewness* close to zero report about symmetric distribution of phase values, which is characteristic for spread and well-adhered cells. Detailed description of these parameters can be found in the Supporting Information. In addition to already mentioned cell parameters, *cell count* in the area of the sample 1 mm^2 and *the confluence* of the cell culture were determined. The confluence is calculated as a ratio of the surface covered by cells. The number of cells together with the level of confluence provides information about the cell proliferation and cell culture viability.

3. Results

3.1. Chemistry of plasma polymerized layers

Previous experiments with CPA plasma polymerization in pulsed radio frequency capacitively coupled discharge using glass tubular reactor showed that the concentration of amine groups is decreasing with increasing power delivered per monomer molecule [22]. Preliminary experiments in stainless steel parallel plate reactor confirmed this trend and three sets of deposition conditions (CPA40, CPA42 and CPA43 in Table 1) were chosen in order to have different amounts of amine groups but similar thickness stability of the films. Regardless of the substrate nature, the deposited CPA plasma polymers uniformly and homogenously covered the surface. The deposition rate was decreasing in the row CPA40 > CPA43 > CPA42 (see Table 1), i.e. an increase of the CPA flow rate and a decrease of the delivered power were enhancing this parameter. Hence, the CPA plasma polymerization was carried out in the monomer deficient regime [45,46]. The FT-IR spectra were similar to the previously reported data of the CPA plasma polymers [20–22]. The spectra revealed the peaks attributed to hydrocarbons, nitriles and amines for all the samples. The intensities of N–H stretching at 3360 cm^{-1} and scissoring at 1640 cm^{-1} as well as the CN peak at 2180 cm^{-1} were the highest for CPA40 whereas the C–H peaks (2960, 2930, 2850 cm^{-1}) were higher in the spectrum of CPA42. Hence, the highest incorporation of amines and nitriles can be expected for CPA40.

The elemental and functional composition of CPA plasma polymer surfaces was characterized by XPS. As shown in Table 2, the highest concentration of nitrogen equal to 19 at.% was estimated for CPA40. The decrease of flowrate and the use of continuous mode led to depletion of nitrogen. This observation is in accordance with recently published results on CPA plasma polymerization in tubular glass plasma reactor in which the substrates were at the floating potential [22]. It was reported that fibroblasts are growing faster on positively charged surfaces [6, 9]. Since amine groups are protonated in aqueous solutions at neutral pH they increase the positive surface charge. Nitriles and amides are neutral moieties not affecting the surface charge. Therefore, it is expected that the concentration of primary and secondary amines played a major role on the cell adhesion, while amide and nitrile functional groups were less important.

In order to quantify the functional composition of the CPA plasma polymers, the XPS C1s and N1s signals were fitted taking into account the FT-IR results and tabulated data of binding energies (BEs) for polymeric materials [35]. The XPS C1s signal was fitted by the sum of three peaks related to hydrocarbons (**C**H_x, BE ~285 eV), carbon singlebonded to oxygen or nitrogen (**C**–O/**C**–N, BE ~286.5 eV) and carbon doublebonded to oxygen (**C**═O, BE ~ 287.9 eV).The N1s signal was fitted by the sum of three nitrogen contributions, namely primary/secondary amines (**N**H_x, BE ~ 399.2 eV), imine/nitride functions (C═**N**, BE ~ 398.3 eV) and amide/nitrile groups (**N**–C═O/C═**N**, BE ~ 400 eV). The example of C1s and N1s curve fitting are shown in Fig. 4 and the percentages of the peaks are reported in Table 3.

Although the **N**H_x environment estimated from the N1s curve fitting cannot be considered as a true concentration of primary and secondary amines, the combination of C1s and N1s curve fitting allow to draw the

Table 2
Atomic composition of the CPA plasma polymers derived from XPS. Atomic percentage of **N**H_x groups was determined by fitting N1s signal (see also Table 3 and Fig. 4).

Sample	C (at.%)	N (at.%)	O (at.%)	**N**H_x (at.%)
CPA40 as deposited	77	19	4	12.3
CPA42 as deposited	81	13	6	6.8
CPA43 as deposited	79	15	6	9.3
CPA40 after 128 h in H_2O	78	13	9	8.1
CPA43 after 128 h in H_2O	79	12	9	7.1

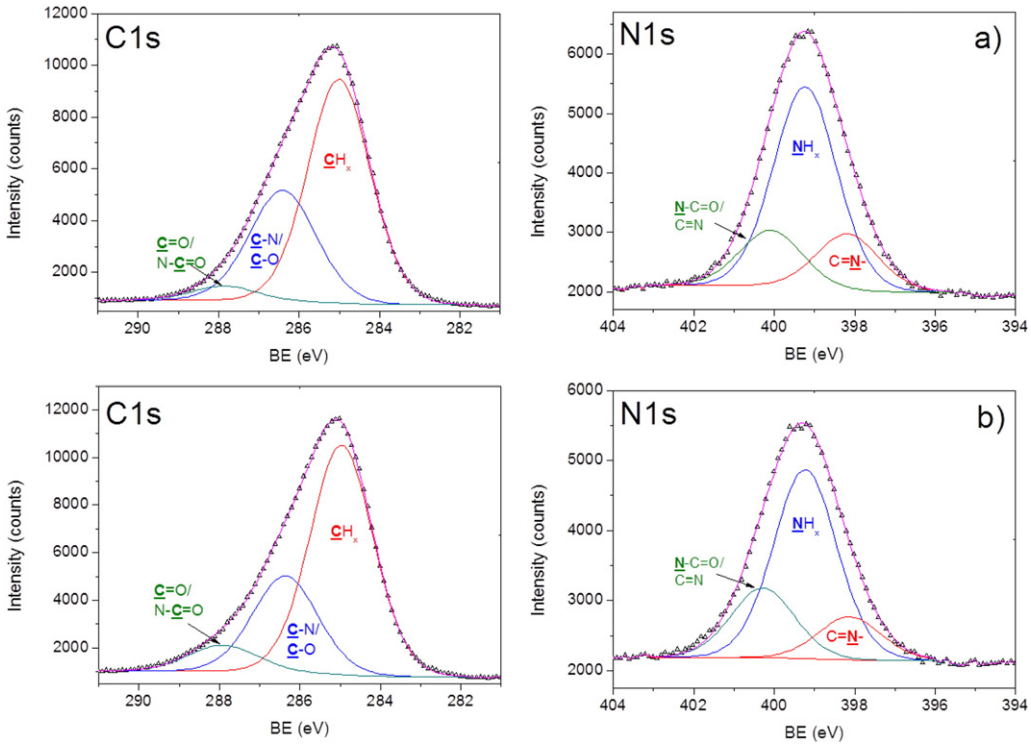

Fig. 4. XPS C1s (on the left) and N1s (on the right) curve fitting of the CPA40 before (a) and after (b) immersion into water.

trend in the surface chemistry changes with plasma parameters. As shown in Table 3, the CPA40 exhibited the highest **C**-N/**C**-O and **N**H_x contributions equal to 25.6 and 12.3 at.%, respectively. Therefore, this layer contains the highest concentration of primary and secondary amines. The decrease of the CPA flow rate led to the decrease of **C**-N/**C**-O and **N**H_x environments down to 21.8 and 9.3 at.%, respectively.By applying the continuous instead of the pulsed plasma, the **C**-N/**C**-O and **N**H_x environments further decreased to 14.4 and 6.8 at.%, respectively. Hence, by tuning the plasma parameters, the layers exhibiting a significantly different concentration of amine groups can be synthesized. However, in order to correctly evaluate the influence of the surface chemistry on the cell adhesion, it is necessary to characterize mechanical properties and water stability of the layers.

3.2. Mechanical properties and water stability of layers

The mechanical properties and water stability of plasma polymers can be very important parameters affecting the cell behaviour. As shown in Table 1, the CPA plasma polymers exhibited very low hardness and elastic modulus. Regardless of soft nature, the thickness loss of CPA40 and CPA43 after 128 h in water was 5.6 and 2.0%, respectively, which is significantly lower compared to the state of the art results of amine plasma polymers exhibiting the same nitrogen content [19,47].

Table 3
The atomic percentages of carbon and nitrogen environments estimated from XPS C1s and N1s curve fitting and atomic composition.

Sample	C1s			N1s		
	CH_x	**C**-N/**C**-O	**C** = O	**N**H_x	**N**-C = O/C ≡ **N**	C = **N**
	(at.%)	(at.%)	(at.%)	(at.%)	(at.%)	(at.%)
CPA40 as deposited	48.4	25.6	3.1	12.3	3.1	3.6
CPA40 after 128 h in H_2O	50.1	21.8	6.2	8.2	3.0	1.8
CPA42 as deposited	60.1	14.4	3.0	6.8	3.9	1.2
CPA43 as deposited	55.7	18.6	4.7	9.3	2.9	2.8
CPA43 after 128 h in H_2O	53.9	18.7	6.5	6.7	3.9	1.4

The hardness of plasma polymers slightly decreased after immersion in water for 24 h, whereas the changes of the elastic modulus were within the experimental errors (Table 1). Despite the low thickness loss, which is 1% only, the layer CPA42 buckled after immersion in water as revealed by CCHM (Fig. 5). Similar behaviour for CPA plasma polymers deposited at high energy per monomer molecule has been already reported for the polymerization in glass tubular reactor [22]. The cell morphology on CPA 42 was highly affected by the layer buckling. Hence, only CPA40 and CPA43 had comparable stability and were further studied concerning properties after water immersion and cell viability.

The XPS analyses of the CPA40 and CPA43 after immersion in water during 128 h revealed the similar increase of oxygen concentration at the expense of nitrogen for both the samples (Table 2). The C1s and N1s curve fitting also highlighted mild changes in the functional composition. The **C** = O/N-**C** = O and **N**-C = O contributions increased at the expense of **C**-N/**C**-O and **N**H_x, respectively. Therefore, a similar oxidation of amine groups towards the amide functions was evidenced for both, CPA40 and CPA43.

3.3. Monitoring of cell behaviour on the plasma-treated surfaces

LF cells seeded on the samples (control, CPA40 and CPA43) were observed and imaged by CCHM. For the visual comparison, the images of the samples with adhered LF cells obtained 4 days after seeding are shown in Fig. 5.S ample CPA43 is not shown due to a visual similarity to the sample CPA40. The sample CPA42 exhibited morphological cracks that affected the behaviour of cells adhered to the surface and caused non-physiological morphology of the cells. For this reason, the sample CPA 42 was discarded from further analyses. The **N**H_x concentration in the sample CPA40 was higher by only 30% compared to CPA43. Unfortunately, a larger variation in the **N**H_x concentration was not possible to achieve because any changes leading to higher or lower **N**H_x alternated the stability of the CPA plasma polymers.

Unlike for CPA42, the LF cells seeded on the control, CPA40 and CPA43 samples indicated a normal behaviour. Nevertheless, the cells

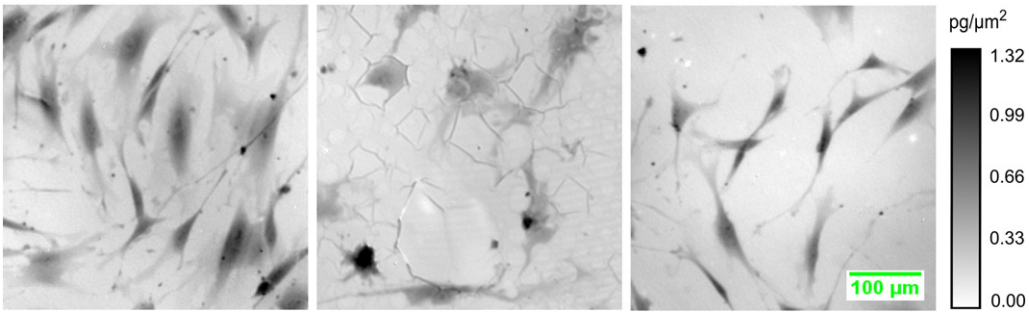

Fig. 5. Quantitative phase images obtained by CCHM (objectives 10×/0.3). LF cells on the CPA40(left), CPA42 (middle) and control (right) sample 4 days after seeding. Scale bar and calibration bar apply to all images.

on the control sample appeared more elongated, thinner and generally less spread in comparison to the samples CPA40 and CPA43. Since only a rough comparison of the cell behaviour between the samples can be attained based on the visual examination, the morphological parameters describing the cell behaviour in a quantitative way were extracted and analysed. It provided additional information that was essential for the comparison of the cell adhesion and proliferation.

The statistical analysis of obtained morphological parameters of the cells together with the confluence and cell count are summarized in Fig. 6. Each bar chart of the particular feature represents the mean value of the parameter for the three samples (CPA40, CPA43 and control) in three time instants (2, 3 and 4 days after seeding). For all the samples, the seeded cells exhibited normal behaviour, indicating the good biocompatibility of all the samples. However, noticeable differences between the samples with different concentration of amine groups on the surface were obvious.

Footprint area (Fig. 6a) together with *total dry mass* of the cells (Fig. 6c) reached significantly higher values in case of samples CPA40 and CPA43 compared to the control. It indicates that the cells on the samples CPA40 and CPA43 are more spread over the surface and have higher overall dry mass compared to the control sample, i.e. exhibit higher viability. *Dry mass density* of the cells (Fig. 6b) and *skewness* of the phase values distribution (Fig. 6d) show that the cells seeded on the sample CPA40 and CPA43 have considerably higher average *dry mass density* and the mass within the cells is more evenly distributed in comparison with the control sample. This informs about the higher level of cell adherence on the two samples. While the four mentioned cell parameters remained unchanged over time for all observed samples, *cell count* (Fig. 6e) and *confluence* (Fig. 6f) demonstrated increasing trend during the time elapsed from the seeding. Such trend was observed for all samples and indicates the normal cell proliferation. However, samples CPA40 and CPA43 demonstrate higher proliferation than the control sample. The differences of the *cell count* and *confluence* values between the samples are more visible from the 3rd day after seeding.

Taking into consideration all the cell morphological parameters, the analysis proved that there are considerable differences between the behaviour of cells seeded on the different surfaces. The CPA40 and CPA43 coatings enhance the cell adhesion and proliferation, i.e. demonstrate higher biocompatibility than the control glass sample. Moreover, the CPA40 showed more significant enhancement regarding most of the monitored parameters than CPA43 against the control, hence exhibits higher biocompatibility. It is in agreement with higher incorporation of amine groups on the surface of this particular sample.

The enhanced adhesion of fibroblasts and endothelial cells to the positively charged surfaces such as amine layers in aqueous media at neutral pH is well known since the 1990s [6,9,48]. Amine groups promote the adsorption of cell adhesion-mediating molecules (e.g. fibronectin, fibrinogen, vitronectin, Arg-Gly-Asp, i.e. RGD peptides) in an appropriate conformation, which is close to the physiological conformation of these molecules [49]. Although the influence of the surface chemistry on the cell adhesion is abundant in the literature, the discussion on the effect of the layer stability is very limited. The results on the sample CPA42 showed how crucial is the layer stability for a normal cell behaviour. Moreover, the live monitoring of the cell behaviour was rarely performed and the cell viability on different surfaces was generally estimated from assays or static single images. Since CCHM enables label-free and quantitative live cell imaging (see Supporting Information, video file), it should be considered as an essential technique for the monitoring of biological reaction of cells to both layer stability and its chemistry.

The deposition of amine coating by plasma polymerization appeared to be an efficient environment friendly method for the preparation of nitrogen-rich biocompatible coatings favouring the adhesion and proliferation of human fibroblasts. Nevertheless, the conditions of plasma polymerization must be carefully tuned to obtain a sufficient amine concentration combined with good layer stability in water. The high plasma power leading to deposition of more compacted films induced not only depletion of NH_x environment but led also to layer buckling induced by contact with water. Such negative effect of plasma power was shown before [22] but requires further analysis to investigate the mechanism of CPA plasma polymer cracking.

4. Conclusion

The plasma polymerization of cyclopropylamine in RF discharge was used as a versatile method for the deposition of thin amine coatings on glass with different concentrations of nitrogen and NH_x groups. Although the surface chemistry can be considered as a crucial parameter, the stability of layers in water strongly affected their biocompatibility. The film with the lowest nitrogen concentration, deposited in the continuous wave mode, cracked when immersed in water. It had detrimental effect on the cell behaviour. Although the films deposited in the pulsed mode were slightly dissolved in water, their morphology did not change and the cells behaved normally. The results from the analysis of human dermal fibroblasts viability by CCHM were correlated with the surface chemistry of the films. It was proved that amine-rich coatings prepared in pulsed plasma are biocompatible and a higher concentration of amine groups at the surface enhances the cell adhesion and proliferation. In the analysis, CCHM played an important role as a reliable technique for monitoring and evaluation of cell–surface interaction without the need of staining and additional sample preparation.

Acknowledgements

This work was supported by CEITEC — Central European Institute of Technology (CZ.1.05/1.1.00/02.0068) from the European Regional Development Fund, by the Specific Research grant of Brno University of Technology (FSI/STI-J-15-2752), and by BioFibPlas project No.

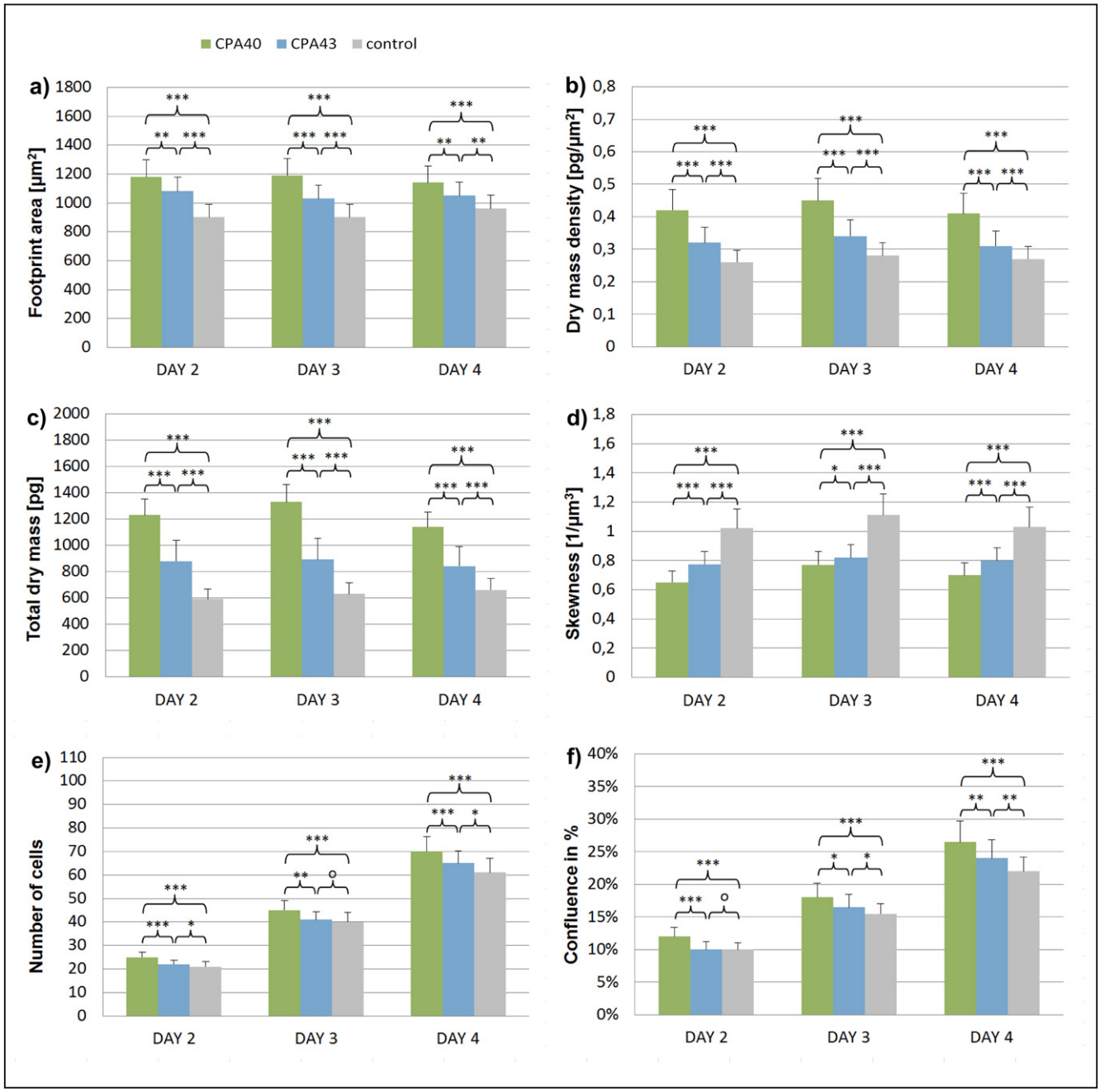

Fig. 6. Morphological cell parameters of cells seeded on the samples CPA40, CPA43 and the control in three time points (2nd, 3rd and 4th days after seeding): (a) footprint area of cells (in μm^2), (b) dry mass density of cells (in $pg/\mu m^2$), (c) total dry mass of cells (in pg), (d) skewness of the phase values (in $1/\mu m^3$), (e) cell count in the area 1 mm^2, (f) confluence of the cell culture (in %). Figure and error bars represent, respectively, mean and standard deviation of the cell parameter values. An unpaired t-test was used for the statistical analysis. Symbols indicating the significance are placed above the figure bars (o: $p > 0.05$, *: $p < 0.05$, **: $p < 0.01$ and ***: $p < 0.001$).

3SGA5652 financed by the SoMoPro II Programme that has acquired a financial grant from the People Programme (Marie Curie Action) of the Seventh Framework Programme of EU according to the REA Grant Agreement No. 291782 and was further co-financed by the South-Moravian Region. This publication reflects only the author's views and the Union is not liable for any use that may be made of the information contained therein.

Appendix A. Supplementary data

Supplementary data to this article can be found online at http://dx.doi.org/10.1016/j.surfcoat.2015.10.076.

References

[1] M. Mihailescu, R.C. Popescu, A. Matei, A. Acasandrei, I.A. Paun, M. Dinescu, Investigation of osteoblast cells behavior in polymeric 3D micropatterned scaffolds using digital holographic microscopy, Appl. Opt. 53 (2014) 4850–4858.
[2] H. Shin, S. Jo, A.G. Mikos, Biomimetic materials for tissue engineering, Biomaterials 24 (2003) 4353–4364.
[3] H. Chen, Z. Zhao, Y. Zhao, Y. Yang, Fabrication and evaluation of chitosan–gelatin based buckling implant for retinal detachment surgery, J. Mater. Sci. Mater. Med. 21 (2010) 2887–2895.
[4] J. Vilches, J. Vilches-Perez, M. Salido, Cell–surface interaction in biomedical implants assessed by simultaneous fluorescence and reflection confocal microscopy, in: A. Méndez-Vilas, J. Díaz (Eds.), Mod. Res. Educ. Top. Microsc. Formatex, Badajoz 2007, pp. 60–67.
[5] M.P. Lutolf, J.A. Hubbell, Synthetic biomaterials as instructive extracellular microenvironments for morphogenesis in tissue engineering, Nat. Biotechnol. 23 (2005) 47–55.

[6] J.H. Lee, H.W. Jung, I.-K. Kang, H.B. Lee, Cell behaviour on polymer surfaces with different functional groups, Biomaterials 15 (1994) 705–711.
[7] K.S. Siow, L. Britcher, S. Kumar, H.J. Griesser, Plasma methods for the generation of chemically reactive surfaces for biomolecule immobilization and cell colonization — a review, Plasma Process. Polym. 3 (2006) 392–418.
[8] A. Makaraviciute, A. Ramanaviciene, Site-directed antibody immobilization techniques for immunosensors, Biosens. Bioelectron. 50 (2013) 460–471.
[9] J.H. Lee, J.W. Lee, G. Khang, H.B. Lee, Interaction of cells on chargeable functional group gradient surfaces, Biomaterials 18 (1997) 351–358.
[10] T.O. Acarturk, M.M. Peel, P. Petrosko, W. LaFramboise, P.C. Johnson, P.A. DiMilla, Control of attachment, morphology, and proliferation of skeletal myoblasts on silanized glass, J. Biomed. Mater. Res. 44 (1999) 355–370.
[11] H. Luo, G. Xiong, K. Ren, S.R. Raman, Z. Liu, Q. Li, C. Ma, D. Li, Y. Wan, Air DBD plasma treatment on three-dimensional braided carbon fiber-reinforced PEEK composites for enhancement of in vitro bioactivity, Surf. Coat. Technol. 242 (2014) 1–7.
[12] K.S. Siow, S. Kumar, H.J. Griesser, Low-pressure plasma methods for generating non-reactive hydrophilic and hydrogel-like bio-interface coatings — a review, Plasma Process. Polym. 12 (2015) 8–24.
[13] M. Moreno-Couranjou, A. Manakhov, N.D. Boscher, J.-J. Pireaux, P. Choquet, A novel dry chemical path way for diene and dienophile surface functionalization toward thermally responsive metal-polymer adhesion, ACS Appl. Mater. Interfaces 5 (2013) 8446–8456.
[14] A. Manakhov, M. Moreno-Couranjou, N.D. Boscher, V. Rogé, P. Choquet, J.-J. Pireaux, Atmospheric pressure pulsed plasma copolymerisation of maleic anhydride and vinyltrimethoxysilane: influence of electrical parameters on chemistry, morphology and deposition rate of the coatings, Plasma Process. Polym. 9 (2012) 435–445.
[15] A. Manakhov, M. Moreno-Couranjou, P. Choquet, N.D. Boscher, J.-J. Pireaux, Diene functionalisation of atmospheric plasma copolymer thin films, Surf. Coat. Technol. 205 (2011) 466–469.
[16] E. Kedroňová, L. Zajíčková, D. Hegemann, M. Klíma, M. Michlíček, A. Manakhov, Plasma enhanced CVD of organosilicon thin films on electrospun polymer nanofibers, Plasma Process. Polym. (2015), http://dx.doi.org/10.1002/ppap.201400235.
[17] D. Duday, C. Vreuls, M. Moreno, G. Frache, N.D. Boscher, G. Zocchi, C. Archambeau, C. Van De Weerdt, J. Martial, P. Choquet, Atmospheric pressure plasma modified surfaces for immobilization of antimicrobial nisin peptides, Surf. Coat. Technol. 218 (2013) 152–161.
[18] B.R. Coad, M. Jasieniak, S.S. Griesser, H.J. Griesser, Controlled covalent surface immobilisation of proteins and peptides using plasma methods, Surf. Coat. Technol. 233 (2013) 169–177.
[19] C. Daunton, L.E. Smith, J.D. Whittle, R.D. Short, D.A. Steele, A. Michelmore, Plasma parameter aspects in the fabrication of stable amine functionalized plasma polymer films, Plasma Process. Polym. 12 (2015) 817–826.
[20] A. Manakhov, D. Nečas, J. Čechal, D. Pavliňák, M. Eliáš, L. Zajíčková, Deposition of stable amine coating onto polycaprolactone nanofibers by low pressure cyclopropylamine plasma polymerization, Thin Solid Films 581 (2015) 7–13.
[21] A. Manakhov, P. Skládal, D. Nečas, J. Čechal, J. Polčák, M. Eliáš, L. Zajíčková, Cyclopropylamine plasma polymers deposited onto quartz crystal microbalance for biosensing application, Phys. Status Solidi A 211 (2014) 2801–2808.
[22] A. Manakhov, L. Zajíčková, M. Eliáš, J. Čechal, J. Polčák, J. Hnilica, Š. Bittnerová, D. Nečas, Optimization of cyclopropylamine plasma polymerization toward enhanced layer stability in contact with water, Plasma Process. Polym. 11 (2014) 532–544.
[23] D. Hegemann, B. Hanselmann, S. Guimond, G. Fortunato, M.-N. Giraud, A.G. Guex, Considering the degradation effects of amino-functional plasma polymer coatings for biomedical application, Surf. Coat. Technol. 255 (2014) 90–95.
[24] S. Michaelis, R. Robelek, J. Wegener, Studying cell-surface interactions in vitro: a survey of experimental approaches and techniques, in: C. Kasper, F. Witte, R. Pörtner (Eds.), Tissue Eng. III Cell-Surface Interact. Tissue Cult. Springer, Berlin Heidelberg 2012, pp. 33–66.
[25] D.J. Müller, Y.F. Dufrêne, Atomic force microscopy: a nanoscopic window on the cell surface, Trends Cell Biol. 21 (2011) 461–469.
[26] G. Popescu, Quantitative Phase Imaging of Cells and Tissues, McGraw Hill, New York, 2011 362.
[27] P. Kolman, R. Chmelík, Coherence-controlled holographic microscope, Opt. Express 18 (2010) 21990–22003.
[28] T. Slabý, P. Kolman, Z. Dostál, M. Antoš, M. Lošťák, R. Chmelík, Off-axis setup taking full advantage of incoherent illumination in coherence-controlled holographic microscope, Opt. Express 21 (2013) 14747–14762.
[29] M. Mir, B. Bhaduri, R. Wang, R. Zhu, G. Popescu, Quantitative phase imaging, in: E. Wolf (Ed.), Prog. Opt. Elsevier 2012, pp. 133–217.
[30] G. Popescu, Quantitative phase imaging of nanoscale cell structure and dynamics, in: L. Wilson, P. Tran (Eds.), Methods Cell Biol. Elsevier 2008, pp. 87–115.
[31] W. Choi, C. Fang-Yen, K. Badizadegan, S. Oh, N. Lue, R.R. Dasari, M.S. Feld, Tomographic phase microscopy, Nat. Methods 4 (2007) 717–719.
[32] M. Mir, Z. Wang, Z. Shen, M. Bednarz, R. Bashir, I. Golding, S.G. Prasanth, G. Popescu, Optical measurement of cycle-dependent cell growth, Proc. Natl. Acad. Sci. U. S. A. 108 (2011) 13124–13129.
[33] B. Rappaz, E. Cano, T. Colomb, J. Kühn, C. Depeursinge, V. Simanis, P.J. Magistretti, P. Marquet, Noninvasive characterization of the fission yeast cell cycle by monitoring dry mass with digital holographic microscopy, J. Biomed. Opt. 14 (2009) 034049.
[34] M. Mohai, XPS MultiQuant: multimodel XPS quantification software, Surf. Interface Anal. 36 (2004) 828–832.
[35] G. Beamson, D. Briggs, High Resolution XPS of Organic Polymers, John Wiley & Sons, Chichester, England, 1992 295.
[36] D. Nečas, I. Ohlídal, D. Franta, Variable-angle spectroscopic ellipsometry of considerably non-uniform thin films, J. Opt. 13 (2011) 85705.
[37] W.C. Oliver, G.M. Pharr, An improved technique for determining hardness and elastic modulus using load and displacement sensing indentation experiments, J. Mater. Res. 7 (2011) 1564–1583.
[38] A. Stoica, A. Manakhov, J. Polčák, P. Ondračka, V. Buršíková, R. Zajíčková, J. Medalová, L. Zajíčková, Cell proliferation on modified DLC thin films prepared by plasma enhanced chemical vapor deposition, Biointerphases 10 (2015) 029520.
[39] R. Chmelík, M. Slabá, V. Kollárová, T. Slabý, M. Lošťák, J. Čolláková, Z. Dostál, The role of coherence in image formation in holographic microscopy, in: E. Wolf (Ed.), Prog, Elsevier, Opt. 2014, pp. 267–335.
[40] T. Kreis, Digital holographic interference-phase measurement using the Fourier-transform method, J. Opt. Soc. Am. A 3 (1986) 847–855.
[41] T. Zikmund, L. Kvasnica, M. Týč, A. Křížová, J. Čolláková, R. Chmelík, Sequential processing of quantitative phase images for the study of cell behaviour in real-time digital holographic microscopy, J. Microsc. 256 (2014) 117–125.
[42] D. Ghiglia, M. Pritt, Two-Dimensional Phase Unwrapping: Theory, Algorithms, and Software, Wiley, New York, 1998 512.
[43] R. Goldstein, H. Zebker, C. Werner, Satellite radar interferometry: two-dimensional phase unwrapping, Radio Sci. 23 (1988) 713–720.
[44] A. Cristoforetti, L. Faes, F. Ravelli, M. Centonze, M. Del Greco, R. Antolini, G. Nollo, Isolation of the left atrial surface from cardiac multi-detector CT images based on marker controlled watershed segmentation, Med. Eng. Phys. 30 (2008) 48–58.
[45] D. Hegemann, Macroscopic investigation of reaction rates yielding plasma polymer deposition, J. Phys. D. Appl. Phys. 46 (2013) 205204.
[46] D. Hegemann, M.M. Hossain, E. Körner, D.J. Balazs, Macroscopic description of plasma polymerization, Plasma Process. Polym. 4 (2007) 229–238.
[47] A. Abbas, C. Vivien, B. Bocquet, D. Guillochon, P. Supiot, Preparation and multi-characterization of plasma polymerized allylamine films, Plasma Process. Polym. 6 (2009) 593–604.
[48] D.Y. Tseng, E.R. Edelman, Effects of amide and amine plasma-treated ePTFE vascular grafts on endothelial cell lining in an artificial circulatory system, J. Biomed. Mater. Res. 42 (1998) 188–198.
[49] N. Faucheux, R. Schweiss, K. Lützow, C. Werner, T. Groth, Self-assembled monolayers with different terminating groups as model substrates for cell adhesion studies, Biomaterials 25 (2004) 2721–2730.